Small Horizontal Axis Wind Turbine Blade Analysis Using CFD

L.D. Rajo*, Sajaq Tenmia[1], E.K. Atanu[2]

[1,2,3]*Department of Mechanical Engineering, International Institute of Research & Technology, INDIA*

Abstract

Blade is very essential part of HAWT (horizontal axis wind turbine). Forces for Lift and drag on the blade has an important role in the wind turbine performance. The main purpose of this work is to perform CFD analysis of a blade and airfoil of wind turbine using k-ω SST model. The lift and drag forces are calculated for the blade at different AOA (angle of attack). For present work the rotor radius is taken 0.690 m, which is a redesigned blade for horizontal axis wind turbine blade. Results obtained from simulation are compared with the experimental work found in literature.

Keywords: Horizontal Axis Wind Turbine, CFD, ANSYS, Airfoil

1. Introduction

Wind turbine rotor interacts with the wind and converts its kinetic energy into usable energy. Atmospheric turbulence produces important various types of aerodynamic forces on wind turbine blade, where turbulence is a primary source of aerodynamic forces on blade of wind turbine. Among the different aspects involved in rotor aerodynamics there are three different approaches that is be applied to analyze the flow around and downstream of a wind turbine that are: field testing, which is highly complex and expensive but provides accurate results; analytical and semi-empirical models, which are not universally reliable; and CFD, which offers the best way to direct measurements.

2. Literature Survey

In the field of CFD, one early attempt to solve numerically the 3-D unsteady Navier-Stokes equations was carried out by Srinivasan and McCroskey (1988). In this paper, the authors used the unsteady thin layer approximation to compute hovering rotor blade flow fields. Also, rotor wake effects were accounted for by applying a correction to the geometric angle of attack of the blades. Later, a rather original approach was tried by Tuncer et al. (1990). In particular, the authors used a velocity-vorticity formulation of the Navier - Stokes equations containing a vorticity transport equation, which is solved in the viscous flow zone, and an integral equation for the velocity. Ekaterinaris et al. (1995) and Srinivasan et al. (1995) published an extensive survey of CFD results on oscillating NACA 0012 and 0015 airfoils when using different types of turbulence models. A quasi-steady approach to unsteady flows based on this methodology has been developed by Cebeci and Jang (1990). In a study of the time averaged pressure and load values, Devinant (2002) showed that the aerodynamic behavior of the airfoil can be greatly affected by the turbulence level, both quantitatively and qualitatively. In particular, a considerable increase in the lift coefficient with the turbulence level was observed. These results were confirmed experimentally by Amandolese and Szechenyi (2004). However, Sicot et al. (2006) found that these effects of turbulence level do not have a significant effect on the power and thrust coefficients of wind turbine.

The effect of rotation on HAWT blades remain incompletely understood and characterized, even though they have been studied extensively. Himmelskamp (1945) investigated for aircraft propellers, the stall delay due to rotation and the increase in lift coefficient. Banks and Gadd (1963) explained the stall delay by the stabilization of the boundary layer against separation due to rotation. Ronsten (1992) compared pressure distributions for rotating and non-rotating blades. He showed significant differences in lift behaviour only at the station farthest inboard on the blade. In Other experimental and numerical studies, Tangler (2004) Le Pape and Lecanu (2004) assumed that 3D effects yield delayed stall (separation nearer the trailing edge for a rotational airfoil) withCl higher than 2D near the blade root location. Timmer and van Rooij (2003) showed that after stall, the values of Cl and Cd depends on the airfoil's leading edge thickness. El-Kasmi and Masson (2008) developed a methodology for simulating the whole flow around the turbine, including the near and the far wake. The proposed method predicts the near-wake region based on knowledge of turbine performance. Sicot et al. (2008) evaluate experimentally the influence of rotation and turbulence on a wind turbine blade aerodynamics, attention particularly on stall mechanisms. Baxevanou et al. (2008) described a new aeroelastic numerical model, which combines a Navier-Stokes CFD solver with an elastic model and two coupling schemes for the study ofthe aeroelastic behavior of blades of wind turbine undergoing classical flutter.

Singh et al. (2011) designed a airfoil for small horizontal axis wind turbines having minimal Reynolds number to achieve better startup and low wind speed performances. To get additional information on the flow characteristics a CFD analysis was also performed. Rajakumar et al. (2011) presented an iterative approach for the determination of aerodynamic performance characteristics of HAWT (horizontal axis wind turbines). The airfoils NACA 4410 and NACA 2415 are taken into consideration for evaluation. Performance analysis was performed with various assumption and CFD analysis of airfoils. Sayed et al. (2012) presented aerodynamic simulations of NREL (National Renewable Energy Laboratory) wind-turbine-blade profiles which is a steady low-speed flow past two-dimensional S-series. Computational Fluid Dynamics (CFD) were used for aerodynamic simulations which is based on the finite-volume approach. It was concluded that the Angle of Attack (AOA) has a dominant effect on determining the optimum profile as compare to the wind speed. Castellani et al. (2013) studied the wind behavior in a complex wind farm of 18 turbines sited in the northern part of Netherlands. For this work Computational Fluid Dynamics (CFD) simulations with actuator disc technique were used. Lee et al. (2014) studied the influence of idealized local shear flows around a two-dimensional airfoil, S809, on its aerodynamic behavior by using CFD simulations. It was found that the shear rate in a flow produce some changes in the lift coefficient but the angle of attack does not have a significant effect.

Mortazavi et al. (2014) worked to achieve a Pareto optimal set of solutions by using a multi-objective genetic algorithm for geometrical characteristics of airfoil sections for 10-meter blades of a horizontal axis wind turbine. A 2D incompressible unsteady CFD solver and the second law analysis were used to evaluate the performance of the airfoil sections during the process of energy conversion. Abu-abrar et al. (2014) performed CFD analysis for design modification and optimization of horizontal axis micro wind turbine blade in order to achieve self rotation without using external aid. Zhu et al. (2014) presented an integrated method for designing airfoil families of large wind turbine blades with the objectives of high Cp and small chord length and conducted a full blade analysis using computational fluid dynamics (CFD). Carrión et al. (2014) presented a tightly coupled CFD–CSD method and its application to two models of wind turbine that are NREL Phase VI and MEXICO wind turbines in order to perform aeroelastic analysis. Aeroelastic effects were found to be a great influence on the larger NREL Phase VI blade as compare to the MEXICO blade. Munir et al. (2015) performed Computational Fluid Dynamics (CFD) in 3-D analysis of aerodynamic forces of a Horizontal Axis Wind Turbine (HAWT) blade and compare with 2-D experimental results. For the analysis of wind blade profile the National Renewable Energy Laboratory (NREL) Phase VI was used as a model. The results were compared with the experimental data for the NREL Phase VI wind turbine blade obtained by NREL at NASA Ames Research Center. 3-D Computational Fluid Dynamics (CFD) simulation was used to calculate and analyze the aerodynamic forces. The commercial ANSYS CFX and parameterized 3-D CAD model of NREL Phase VI were used for the analysis. It was concluded that the 3-D analysis of aerodynamic force of blade surface it is better to use NREL 3-D values instead of 2-D experimental values.

Heo et al. (2016) designed a horizontal axis wind turbine blade for 110 kW power output and CFD analysis is carried out at different wind speed and flow angle for the 110 kW BAWT (Building augmented wind turbine) with various reference. Li et al. (2016) presented the turbulent wake characteristics of the Horizontal Axis Wind Turbine (HAWT) by comparing the results between the model fitted and wind tunnel experiments. By comparing the results of wind tunnel experimental and numerical analysis, it was found that recovery of wind velocity and expansion of wake deficit area were promoted by turbulence of inflow which was generated by active turbulence grids.

The analysis of HAWT blade aerodynamics is necessary to take into consideration the combined effects of rotation and turbulence. In the present literature this problem is not well recognized. Initial research in this area is concerned with the influence of turbulence on an airfoil of wind turbine blade. This work is the extension of the work done by Tenguria et al. (2010) in which heredesigned a blade for VESTAS V82-1.65 MW HAWT based on optimal rotor theory and carried out structural analysis.

In the present work, the shear stress transport (SST) k-ω model is used which involve a damped cross-diffusion derivative term ω in equation. The SST k- model is as equal as k-ω model but the turbulent viscosity is adapted for purpose of the transport of

the turbulent shear stress. The flow on wind turbine blade is generally separated because of high angle of attack which again depends on turbulence level, tower misalignment or shadow. The present work is focused on the influence of turbulence on the wind turbine blade airfoil. The boundary layer is always unsteady, inhomogeneous and turbulent which is passing through a wind turbine blade and also consisting of pressure fluctuations and quick velocity. The k-ω based SST model was chosen as it gives highly accurate predictions of the onset and the amount of flow separation under adverse pressure gradients. The SST model is recommended for high accuracy boundary layer simulations. Correlation with other types of models is not the part of this work. If we compare this work with the work of Chandrala et al. (2012) as they worked on different airfoil NACA 4420. This work includes the static pressure contour at various angle of attack and plots for pressure distribution at different positions.

3. Governing Equations

The continuity equation for the two dimensional, steady and incompressible flow is:

$$\nabla . (\rho V) = \frac{\partial(\rho u)}{\partial x} + \frac{\partial(\rho v)}{\partial y} = 0 \tag{1}$$

For viscous flow in x direction the momentum equation is:

$$\rho \frac{Du}{Dt} = \frac{\partial \rho}{\partial x} + \frac{\partial \tau_{xx}}{\partial x} + \frac{\partial \tau_{yx}}{\partial y} + \frac{\partial \tau_{zx}}{\partial z} + \rho \int_x \tag{2}$$

Where due to characteristics of the two dimensional flow in continuity equation the term $\frac{\partial() \rho w}{\partial z}$ and in momentum equation,

$\frac{\partial \tau_{zx}}{\partial z}$ drop out. In all simulations a standard k-ω SST model has been used for turbulent viscosity.

In equation

ρ	= Density of fluid
V	= Velocity vector
ρV	= Mass flux
∇	= Vector operator
$\nabla . (\rho V)$	= Divergence of ρV
$\rho u, \rho v$	= Rate of mass entering in x, y direction respectively
τ	= Shear stress
f_x	= External force
$\rho \dfrac{Du}{Dt}$	= Substantial time derivative of velocity
u	= Velocity vector in x direction.

4. Boundary Condition and Geometry

In present analysis, an airfoil from the 6 series of NACA laminar wing section family is used. The airfoil maximum relative thickness is 21%, which is situated at 35% of the chord length. for angles of attack (AOA) ranging from -2 to 10 degrees, because of greater reliability of both computed and experimental values in this region. The selected airfoil profile has 50 no. vertices and it is created in ANSYS GUI 12.0 with two edges upper and lower. The mesh is generated in ANSYS workbench 12.0 and then boundary conditions are applied using ANSYS Fluent 12.0. Figure 1 is showing the airfoil profile of NACA. Once the airfoil edges were

created then boundary layers are generated around the airfoil. Generally , the dimensions of the fluid domain can be presented as show n in Figure 2-A as recommended by Vestas India. Another 3D model was created to asses the front velocities and pressure, the fluid domain was used in the analysis is shown in Figure 2-B.
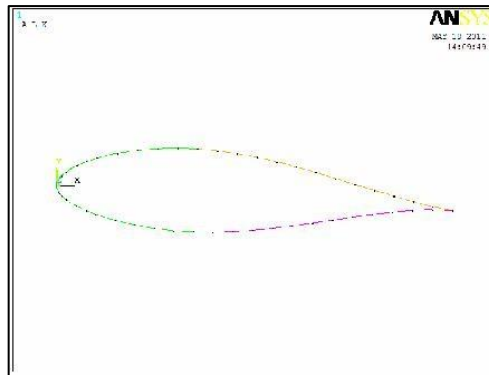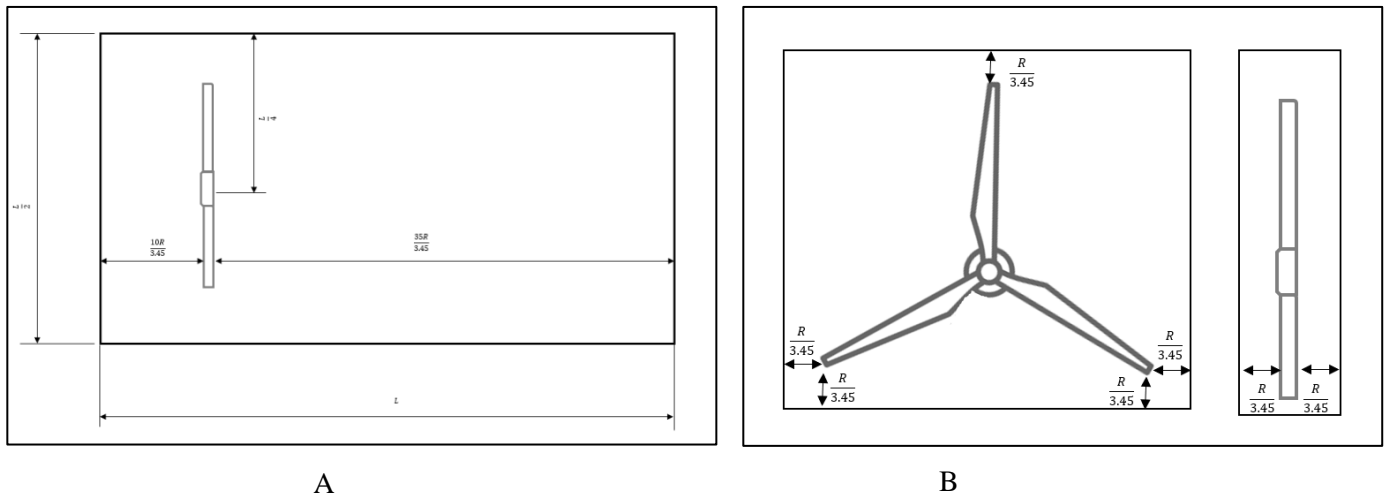

Figure 1. NACA Airfoil Profile

A	B

Figure 2. Dimensions of Fluid Domain A) 2D, B) 3D

5. Results

The XY plots for pressure distribution on top and lower surface is shown in figure 15 to 20. In this case the shock wave is not much strong and the Mach number is not high. But on the other hand the shock wave has got considerable effects up to small extent on pressure distribution.

Advantage Materials Letters (AML)

Vol.38, No, 1 Aug 2018
Vbbripress.org
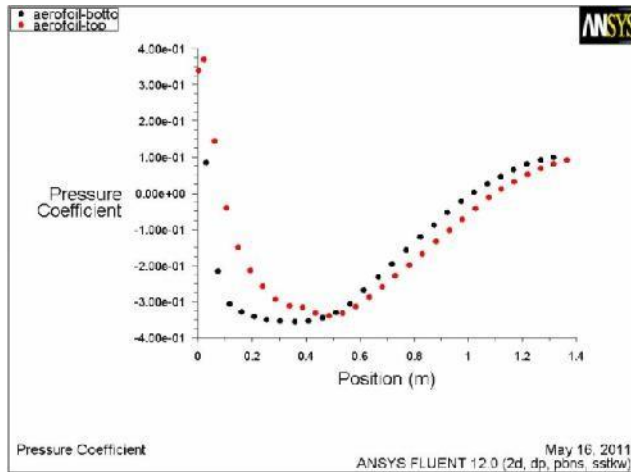
Figure 3. Pressure coefficient plot at -2°
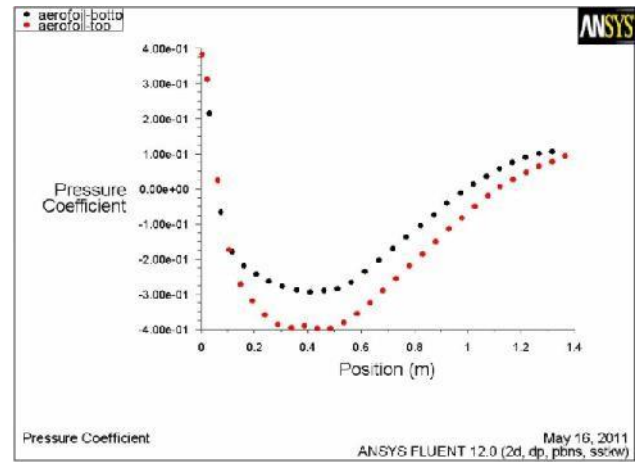
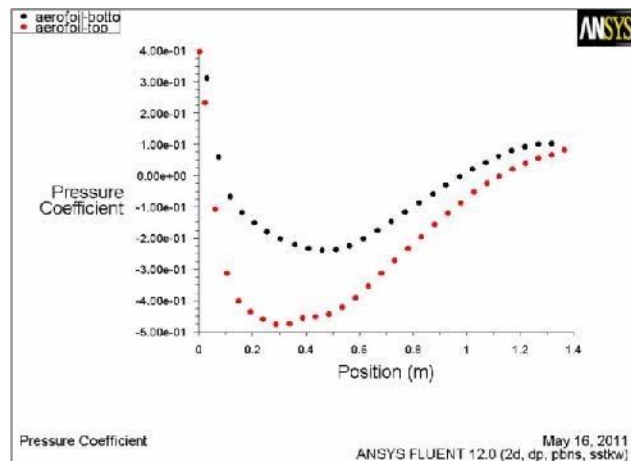**Figure 4** Pressure coefficient plot at 0°

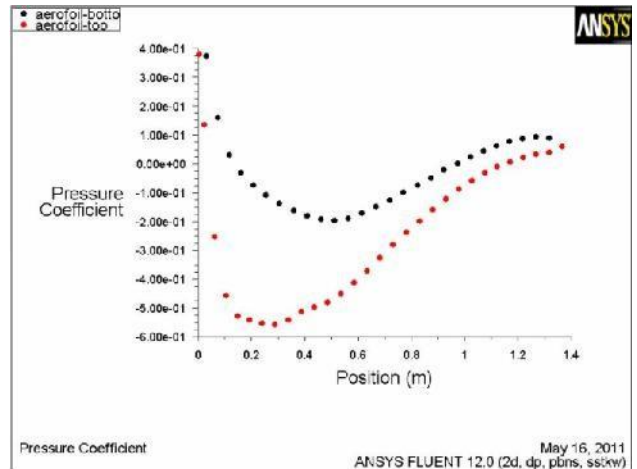**Figure 5.** Pressure coefficient plot at 2°

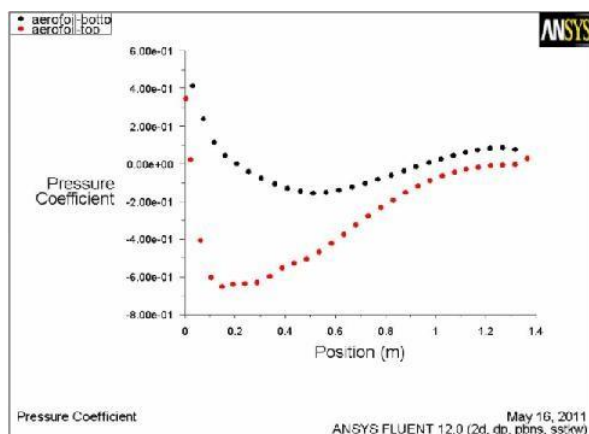**Figure 6**. Pressure coefficient plot at 4°
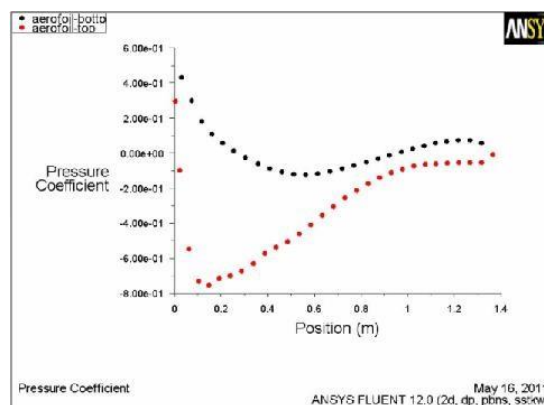
Figure 7. Pressure coefficient plot at 6°

Figure 8. Pressure coefficient plot at 8°

The components of x shock wave on top surface of airfoil are shown in figure 9 to 10. The observation of Mach number or velocity distribution over the airfoil surface, the variation of the x component of the shock wave along the top and bottom surface of the airfoil could be justified.
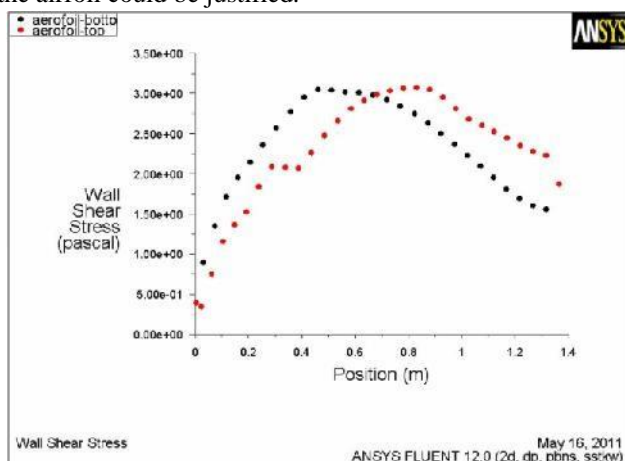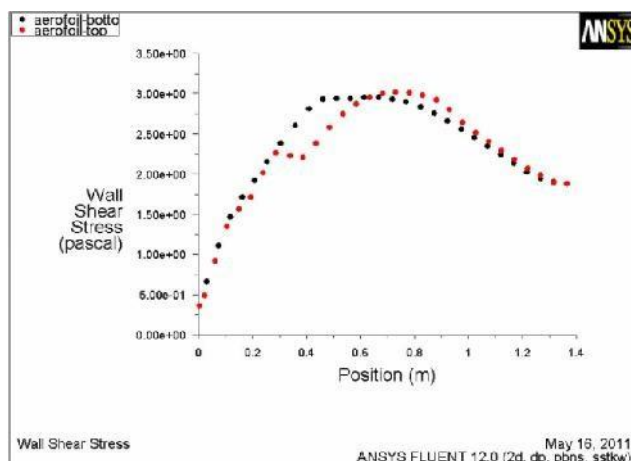

Figure 9. Wall shear stress plot at -2°
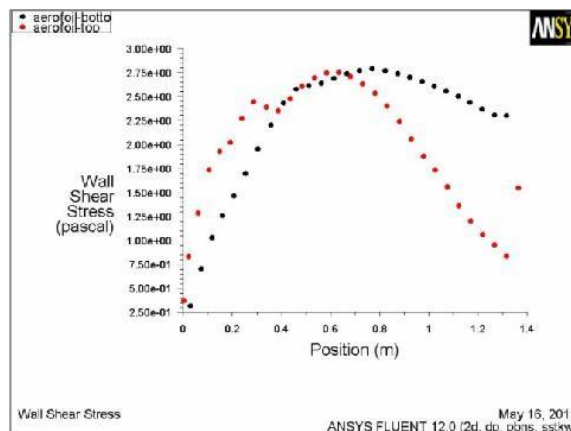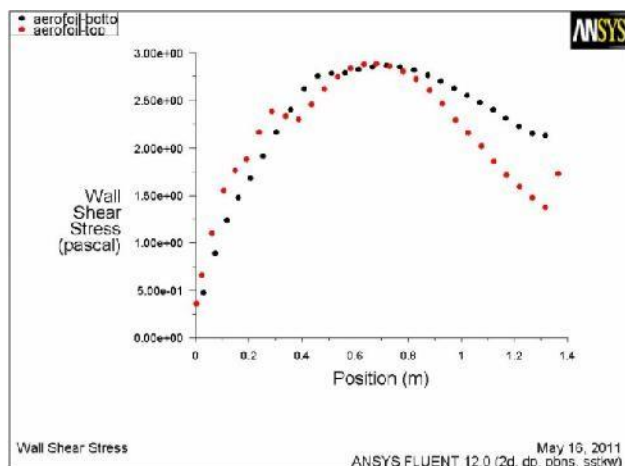

Figure 10. Wall shear stress plot at 0°
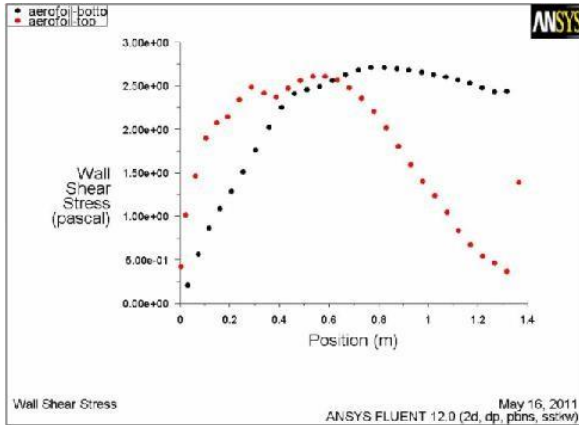
Figure 11. Wall shear stress plot at 2°

Figure 12. Wall shear stress plot at 4°

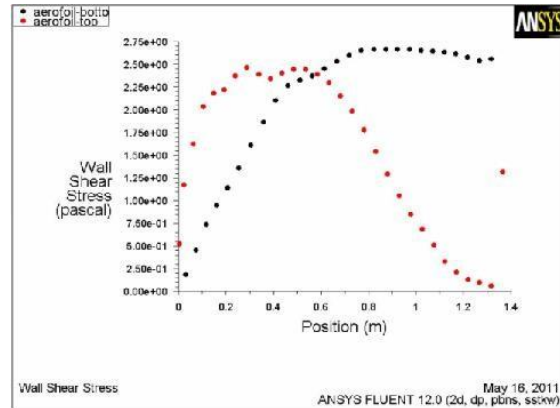**Figure 13.** Wall shear stress plot at 6°

Figure 14. Wall shear stress plot at 8°

Comparison of simulation and experimental results

There are two forces and one moment works on an airfoil. The force component which is normal to the incoming flow stream is known as lift force and the component which is acting parallel to the flow stream is known as drag force. In this analysis, first of all simulation is carried out and then for purpose of validation simulated results are being compared with experimental results as per [Summary of Airfoil Data by H. Abbott et al.]. Here simulation is done for angle of attack -2 to 8°.

Distribution of pressure on both sides top and bottom, contributes to the lift. Pressure drag is the part of drag force connected to the pressure distribution around the airfoil. Skin friction drag is the part of drag force connected to the viscous stresses and form drag is the sum of total stresses. Figure 15 shows the variation of drag coefficient w.r.t. angle of attack, where it is observed that the drag coefficient increases from -2° to 6° but the manner is not linear and the same pattern is observed with a slight difference in experimental and simulation results. After angle of attack 6° the drag coefficient varies linearly and approaches its maximum value at angle of attack 8° and there is a very slight difference between experimental and simulation results for this region.
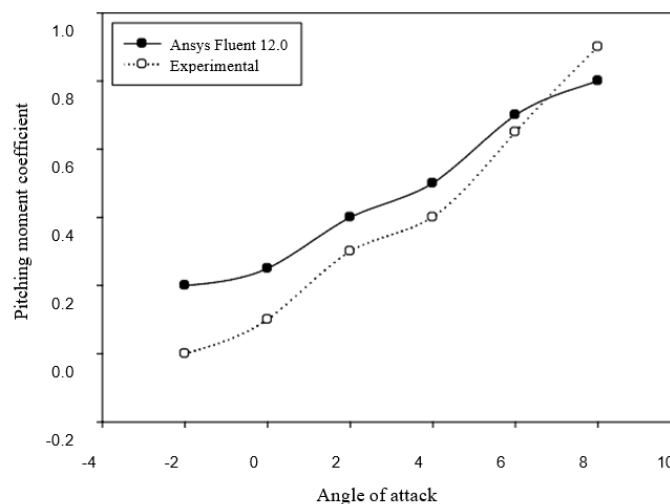

Figure 15. Pitching moment coefficient

Advantage Materials Letters (AML)

Conclusion

   In this work CFD analysis of wind turbine blade is done in ANSYS Fluent 12.0. For this analysis k-ω SST model is used for obtaining lift coefficient, drag coefficient and pitching moment at different angles of attack. The results obtained from simulation are compared with experimental results found in literature. It is found that lift coefficient, drag coefficient and pitching moment increases with increase in angle of attack. It is also found that the pressure at lower surface of airfoil is more and velocity is higher on the upper surface of airfoil.

Nomenclature

CFD   Computational Fluid Dynamics
HAWT   Horizontal Axis Wind Turbine

References

Abbott I.H., Von Doenhoff A.E., Stivers L., NACA Report No. 824 – Summary of Airfoil Data, *National Advisory Committee for Aeronautics.*

Abrar M. A., Mahbub I.A M, Mamun M. 2014. Design optimization of a horizontal axis micro wind turbine through development of CFD model and experimentation. *Procedia Engineering,* Vol. 90, pp. 333-338.

Amandolese X., Szechenyi E., 2004. Experimental study of the effect of turbulence on a section model blade oscillating in stall. *Wind Energy,* Vol. 7, pp.267–282.

ANSYS FLUENT 6.3, *User's Guide, Fluent Inc.*, Feb. 2006.

ANSYS FLUENT 12.0, *User's Guide, Fluent Inc.*, Feb. 2009.

Banks W., Gadd G., 1963. Delaying effect of rotation on laminar separation. *AIAA Journal* 1, pp.941-942.

Baxevanou C.A., Chaviaropoulos P.K., Voutsinas S.G., Vlachos N.S. 2008. Evaluation study of a Navier– Stokes CFD aeroelastic model of wind turbine airfoils in classical flutter. *Journal of Wind Engineering and Industrial Aerodynamics* 96, pp.1425-1443.

Chandrala M., Choubey A., Gupta B. 2012. Aerodynamic analysis of horizontal axis wind turbine blade. *International Journal of Engineering Research and Applications,* Vol. 2, No. 6, pp.1244-1248

Castellani F., Gravdahl A., Crasto G., Piccioni E., Vignaroli A. 2013. A practical approach in the CFD simulation of off-shore wind farms through the actuator disc technique. *Energy Procedia, Vol.* 35, pp.274-284

Carrion M., Steijl R., Woodgate M., Barakos G.N., Munduate X., Gomez-Iradi S 2014. Aeroelastic analysis of wind turbines using a tightly coupled CFD–CSD method. *Journal of Fluids and Structures,* Vol. 50, pp.392-415.

Cebeci T., Jang H.M. 1990. Interactive boundary-layer method for unsteady airfoil flows: quasi steady model, *Journal of Aircraft.* Vol. 27, No. 8, pp.673-678.

 Devinant P., Laverne T., Hureau J 2002. Experimental study of wind-turbine airfoil aerodynamics in high turbulence. *Journal of Wind Engineering and Industrial Aerodynamics,* Vol. 90, pp.689-707.

Ekaterinaris J.A., Srinivasan G.R., McCroskey W.J. 1995, Present capabilities of predicting two dimensional dynamic stall, Aerodynamics and Aeroacoustic Rotorcraft *AGARD-CP*-552, pp.2/1–2/23.

El- Kasmi A., Masson C. 2008. An extended k-ε model for turbulent flow through horizontal-axis wind turbines.
   Journal of Wind Engineering and Industrial Aerodynamics, Vol. 96, pp.103-122.

Heo Y.G., Choi N.J., Choi K.H., Ji H.S. and Kim K.C. 2016. CFD study on aerodynamic power output of a 110 kW building augmented wind turbine. *Energy and Buildings,* Vol. 129, pp.162–173.

Himmelskamp H., 1945. Profile investigations on a rotating airscrew. Germany, Gottingen.

Le Pape, A., Lecanu J., 2004. 3D Navier–Stokes computations of a stall-regulated wind turbine. *Wind Energy,* Vol. 7, pp.309-324.

Lee K.S., Chung C.H., Baek J.H. 2014, Lift correction model for local shear flow effect on wind turbine airfoils, *Renewable Energy,* Vol. 65, pp.275-280.

Li Q., Murata J., Endo M., Maeda T., Kamada Y. 2016. Experimental and numerical investigation of the effect of turbulent inflow on a horizontal axis wind turbine (Part II: Wake characteristics). *Energy,* Vol. 113, pp. 1304-1315.

Munir N.B., Lee K., Huque Z. and Kommalapati R.R. 2015. A study of aerodynamics force evaluation of horizontal axis wind turbine (HAWT) blade using 2D and 3D comparison. *ASME 2015 Power Conference collocated with the ASME 2015 9th International Conference on Energy Sustainability, the ASME 2015 13th International Conference on Fuel Cell Science, Engineering and Technology, and the ASME 2015 Nuclear Forum, ASME 2015 Power Conference,* ISBN: 978-0-7918-5660-4.

Mortazavi S.M., Soltani M.R., Motieyan H. 2014. A Pareto optimal multi-objective optimization for a horizontal axis wind turbine blade airfoil sections utilizing exergy analysis and neural networks. *Journal of Wind Engineering and Industrial Aerodynamics*, Vol. 136, pp.62–72.

Rajakumar S., Ravindran D. 2011 Iterative approach for optimising coefficient of power, coefficient of lift and drag of wind turbine rotor. *Renewable Energy,* Vol. 38, pp.83-93

Ronsten, G., 1992. Static pressure measurements on a rotating and a non-rotating 2.375m wind turbine blade. Comparison with 2D calculations. *Journal of Wind Engineering Industrial Aerodynamics,* Vol. 39, pp.105–118.

Sayed M.A., Kandil H.A., Shaltot A. 2012. Aerodynamic analysis of different wind-turbine-blade profiles using finite-volume method. *Energy Conversion and Management,* Vol. 64, pp.541-550.

Sicot C., Aubrun, S., Loyer S., Devinant P., 2006. Unsteady characteristics of the static stall of an airfoil subjected to freestream turbulence level up to 16%. *Experimental Fluids,* Vol. 41, pp.641–648.

Sicot C., Devinant P., Loyer S., Hureau J. 2008. Rotational and turbulence effects on a wind turbine blade. Investigation of the stall mechanisms. *Journal of Wind Engineering and Industrial Aerodynamics,* Vol. 96, pp.1320– 1331.

Singh R.K., Ahmed M.R., Zullah M.A., Lee Y.-H. 2011. Design of a low Reynolds number airfoil for small horizontal axis wind turbines. *Renewable Energy,* Vol. 42, pp.66-76

Srinivasan G.R., McCroskey W.J. 1988. Navier–Stokes calculations of hovering rotor flow fields, *Journal of Aircraft,* Vol. 25, No. 10, pp. 865-874.

Srinivasan G.R, Ekaterinaris J.A., McCroskey W.J. 1995, Evaluation of turbulence models for unsteady flows of an oscillating airfoil, *Computational Fluids,* Vol. 24, No. 7, pp.833–861.

Tangler J.L., 2004. Insight into wind turbine stall and post-stall aerodynamics. *Wind Energy,* Vol. 7, 247–260.

Tenguria N., Mittal N.D., Ahmed S. 2010. Design and finite element analysis of horizontal axis wind turbine blade. *International Journal of Applied Engineering Research,* Vol. 1, No. 2, pp.500-507.

Timmer W.A., van Rooij R., 2003. Summary of the Delft university wind turbine dedicated airfoils. *AIAA journal*-0352.

Tuncer I.H., Wu J.C., Wang C.M. 1990. Theoretical and numerical studies of oscillating airfoils, *AIAA Journal,* Vol. 28, No. 9, pp.1615-1624.

Zhu W.J., Shen W. Z., Sorensen J. N. 2014. Integrated airfoil and blade design method for large wind turbines. *Renewable Energy,* Vol. 70, pp. 172-183.